NON-DESTRUCTIVE EXPERIMENTATION: DYNAMIC IDENTIFICATION OF MULTI-LEAF MASONRY WALLS DAMAGED AND CONSOLIDATED

Authors:

Giosuè Boscato[1], Emanuele Reccia[2], Antonella Cecchi[3]

[1] gboscato@iuav.it, LabSCo Construction Sciences Lab, Università IUAV di Venezia, via Torino 153/A, 30172, Venice, Italy

[2] emanuele.reccia@uniroma1.it, Department of Structural and Geotechnical Engineering (DISG), Sapienza, University of Rome, via A. Gramsci 53, 00197 Rome, Itlay

[3] cecchi@iuav.it, Department of Architecture Construction Conservation (DACC), Università IUAV di Venezia, Dorsoduro 2206, 30123 Venice, Italy

Submitted to: **Composites Part B: Engineering** - DOI:10.1016/j.compositesb.2017.08.022

ABSTRACT

The dynamic monitoring of multi-leaf masonry wall is here proposed. The results of non-destructive tests carried out in this work are a first part of a wider testing campaign aimed at verifying the structural performance of masonry walls. Multi-leaf masonry walls constitute the composite construction typology most widely adopted in historic buildings. This aspect, together with the intrinsic structural complexity, heterogeneity and irregularity, directs the present research towards a topic not yet sufficiently investigated by the scientific community. In this paper, the case of multi-leaf masonry wall has been investigated, and with the aim of reproducing historical buildings structural elements, three different typologies of multi-leaf masonry walls have been considered: (i) full infill, (ii) damaged infill, (iii) consolidated infill.

Several masonry specimens of the above described typologies have been built and tested in lab. The dynamic parameters, such as frequencies, modal shapes and damping ratios have been identified through the output-only procedure and the data were processed through the Least Square Complex Frequency (LSFC) estimator; the analysis of results allowed to evaluate the structural integrity, the efficacious of consolidating intervention and the potential performance mechanisms of different complex multi-leaf masonry walls.

Experimental results are compared with numerical Finite Elements models. Composite multi-leaf masonry is modelled as an equivalent continuum obtained through a full 3D homogenization procedure. The mechanical properties of component materials have been obtained in lab by tests and then used to model the masonry at the micro-scale in order to derive the

mechanical properties to be adopted at macro-scale. A parametric natural frequencies analysis is performed in order to calibrate the model by the comparison whit the experimental measures.

Keywords: *Dynamic Identification, Multi-leaf Masonry Walls, D. Non-Destructive Testing, C. Finite Elements Analysis, B. Mechanical properties.*

1. **INTRODUCTION**

Multi-leaf masonry walls constitute a widely spread construction technology of historical masonry bearing composite walls. They are made by two separate external regular masonry panels interconnected by filling the internal cavity with a mixture of mortar and cobblestones, generating a monolithic structural element. Between the various historical wall typologies, multi-leaf walls are among the most difficult to describe in structural terms, due to their constructive features as well as their complex structural behavior.

The term multi-leaf covers a big variety of constructive typologies: from walls made of two exterior panels and a very small internal leaf – which may rather be considered as a vertical joint – to very thick walls – up to one meter – in which the bearing capacity is principally ensured by the internal leaf, whereas the two external panels constitute the formwork, which enabled the construction process. Between those two limits, a variety of multi-leaf walls may exist, the most common is the three-leaves wall made by two external bearing panels and in internal core made by mortar and a mix of waste from the construction yard – brick potsherds, broken shingles, stones, gravel, etc.

The different mechanical properties of the composite leaves, the manufacturing imperfections and unknowns and the difficulty of describing the conditions at the interface between the external walls and the internal core make the study of their structural behavior a complex issue. Both local and global behavior of multi-leaf masonry walls are affected by the mechanical characteristics of the materials, the structural interaction between the leaves, the geometric configuration, the size effect, the thickness of mortar and the manufacturing technology [1]. Main structural problems are related to the weakness of the internal core and the lacking of the connection between the leaves. As a consequence, multi-leaves walls are very sensitive to brittle collapse mechanisms, which usually happen, both under vertical and horizontal loads, by the detachment of the layers and out-of-plane expulsions. The quality of the internal fill – compact filling, distribution of mortar, presence of voids – and the interface between the leaves determines whether there exists a “collaboration” between them. Being the stiffness of external walls and internal core usually very

different, the load transfer is possible through shear mechanisms, it depends by cohesion and friction that characterize the interface between the leaves.

Considering the difficulties in the structural assessment and the wide diffusion, the study of the behavior of multi-leaves walls is of great interest in the fields of structural engineering and conservation of historical architectural heritage. The correct evaluation of their mechanical behavior and the adoption of structural models able to describe it are open issues. However, at present only few studies are available in the technical literature concerning this topic, usually limited to laboratory specimens [2, 3, 4, 5, 6] or panels of small dimensions [7, 8]. Vintzileou [9] proposes simple formulae to asset the compressive strength of three-leaf masonry after grouting. Different configurations of strengthened three-leaf stone masonry walls have been analyzed by Silva et al. [10, 11] and Valluzzi et al. [12], considering injections, repointing and ties connecting. Other researches about this topic have been carried out by Egermann [13], Drei and Fontana [14] and Pina-Hernandez with other authors [15]. Structural models for the limit analysis of multi-leaf walls have been proposed by Milani [16, 17].

Here attention is paid to the dynamic structural identification of multi-leaf masonry walls. This work is part of a wider research project devoted to the mechanical characterization of multi-leaf masonry walls by means of experimental tests and numerical analyses. Several specimens of multi-leaf masonry walls have been built and tested in laboratory. During compressive tests dynamic measures have been collected, with the twofold purpose of calibrate the numerical models by means of dynamic identification and of evaluate the dynamic behavior of the walls at increasing of the damage. In this phase, the attention is focused to the calibration of the models, thus the measure considered have been collected at the beginning of the tests, at a very low value of the load when the specimens were still not damaged.

The dynamic identification of masonry wall is a procedure not yet sufficiently investigated. This monitoring methodology is widely applied to building [18, 19], while few researches have been carried out on single masonry walls. Giaretton [20] analyzes the out-of-plane dynamic response of multi-leaves masonry walls trough shaking table test; while Ramos [21] applies the vibrational analysis for the damage identification of masonry structured base to simulate the masonry piers under the earthquake actions. The dynamic identification were carried out by means the output-only and the data were processed through the Least Square Complex Frequency (LSFC) estimator by LMS Polymax algorithm [22]. The experimental modal analysis has been used to identify the dynamic parameters, such as the natural frequencies, the modal shapes and the damping ratio. Considering the complex configuration of multi-leaf masonry walls both sides have been monitored in order to identify the local, the uncoupled and the global modal shapes; in detail the

first is due to the intrinsic imperfection of masonry wall, while the second and then the third to the effectiveness of the infill.

The dynamic identification is performed on three different types of multi-leaf masonry specimens: (i) full infill, (ii) damaged infill, (iii) consolidated infill (see Section 2). Tests have been performed at the LabSCo (*Laboratorio di Scienza delle Costruzioni, Laboratory of Strength of Materials*), University IUAV of Venice, Italy. Moreover, a series of preliminary tests have been carried out in order to characterize the mechanical properties of material components [23]. The masonry panels tested in laboratory have been reproduced by means of Finite Element models. Models will be used to investigate the behavior of multi-leaf masonry walls and in particular to evaluate the role played by the infill, as well as the other aspects that affect the structural behaviour of different configurations. Whit this purpose, the correct calibration of the models is needed: the comparison between experimental and numerical results is essential to tune the models. At beginning, the mechanical properties adopted in the numerical model are taken from the experimental results on materials component. A full 3D standard homogenization procedure [24, 25] is adopted to derive equivalent continua parameters for modeling external masonry leaves. After, the mechanical parameters have been calibrated on the entire masonry walls on the base of dynamic measures. The targets is the evaluation of the reliability of the continuous models proposed to take into account the complexity of multi-leaf configuration and to describe their behavior.

2. MASONRY SPECIMENS

For the compressive tests, 9 masonry multi-leaf specimens were built considering 3 different typologies of infill: i) full (B1); ii) damaged (B2); iii) consolidated (B3), see Figure 3 [23]. For the construction of masonry specimens, standard clay bricks (Danesi DM 116, UNI 12.6.25) were used, while the mortar used for layers, joints and infills, was specially produced in order to simulate a historic mortar with very low shear strength (Tassullo 14303 CP/5), *(Note: all references are made to a manufacturer's product for the purposes of factual accuracy. No endorsement is implied)*. Masonry specimens have dimensions (1.44x1.42x0.38) m^3 and they are constituted by 22 brick layers. Geometric description of specimens is reported in Fig. 1. On the bottom and on the top of each wall, 2 masonry layers are assembled in order to ensure the infill integrity. Moreover, for those layers, cement mortar reinforced by steel textile net has been used to allow an easy specimens movement in lab. In order to guarantee equally uniform distribution of the loads, during compressive tests, bottom and top of the specimens have been refinished by cement mortar.

For the first typology, the infill has been done with bricks potsherds and mortar CP/5 (B1 of Figure 2). The same infill has been adopted also for the other typologies for 2/3 of the whole mass.

In case of damaged infill typology, only bricks potsherds constitute the central part (B2 of Figure 2), while for the consolidated typology (B3 of Figure 2), the same part has been strengthened by a consolidating mixture.

Different types of mortar have been used during specimens construction. A special type of mortar has been created in collaboration with Tassullo Materiali S.p.A., in order to simulate a historic hydraulic lime mortar, namely type CP/5. This mortar has been used in the construction of masonry specimens both for joints and for the infill. Other two typologies of mortar (TD 13 C and TD 13 SRG) with higher structural performance have been used for the top and bottom layers of masonry specimens.

For the laboratory tests on mortars, all specimens were prepared in accordance to the EN 1015-11. The average values of the mechanical characteristics obtained by flexural and compressive tests are reported. In detail, the average values of the flexural strength (f_{tm}) are for CP/5=0.33MPa, TD13C=1.859MPa, TD13SRG=2.571MPa; while for the average compressive strength (f_{cm}) the values are for CP/5=1.162MPa, TD13C=9.024MPa, TD13SRG=6.539MPa.

The compressive tests on brick samples have been carried out on standard bricks, Danesi DM 116, UNI 12.6.25. The tests were performed on 3 specimens determining a mean value of elastic modulus equal to 4100MPa. For the determination of initial shear strength nine specimens were prepared in accordance to EN 1052-3. The tests were performed without pre-compression. The average value of the shear strength is equal to 0.187MPa.

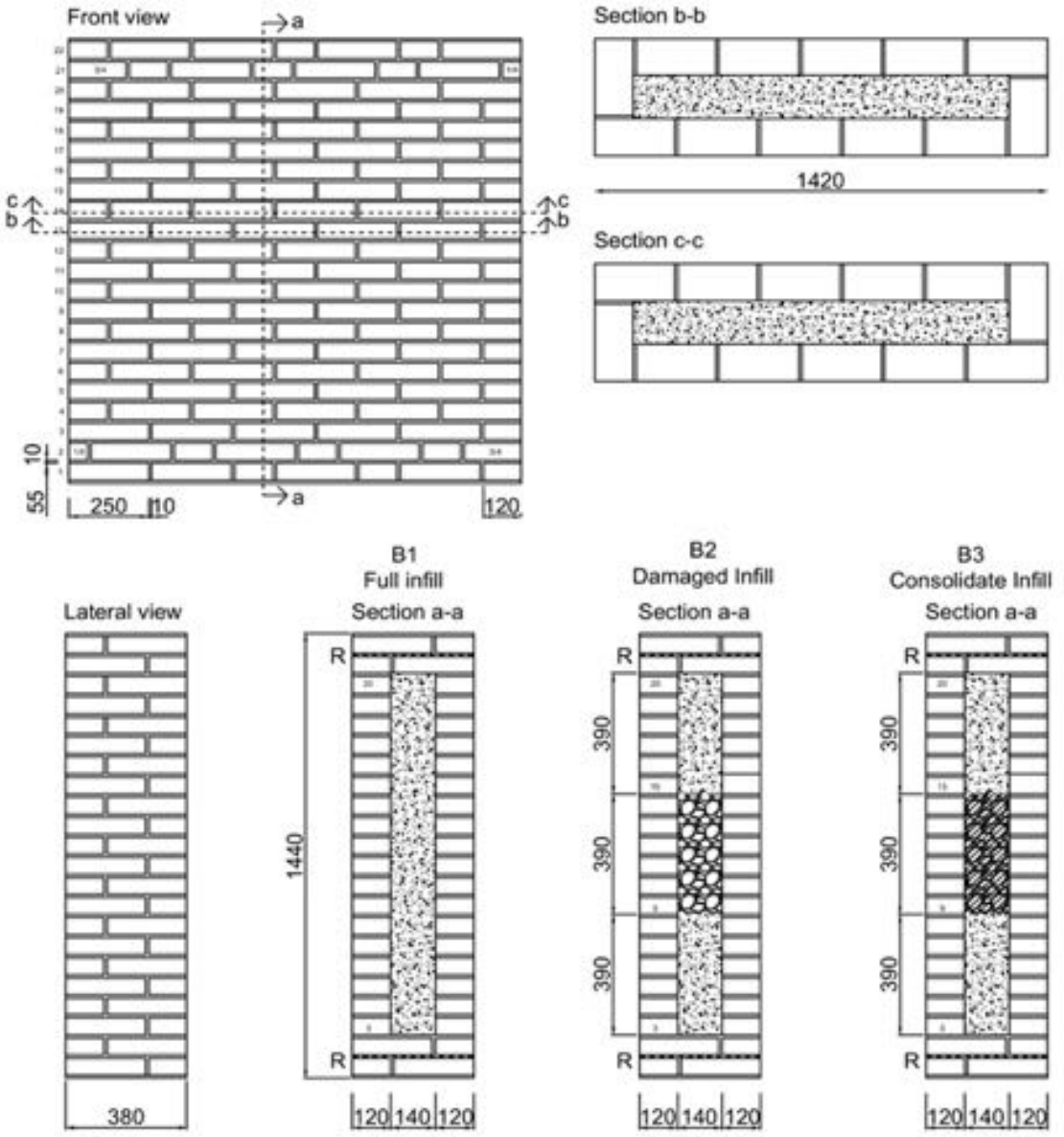

Fig. 1. Masonry specimens.

Fig. 2. Construction phases of masonry specimens.

Figure 3 shows the test setup during the vibration test at initial conditions without the load applied. The accelerometer sensors were applied along the horizontal and vertical barycentric directions for both side in order to recorder the main bending and torsional modal shapes. The accelerometer sensors positioned at the corner, P1 and P7, have monitored the edge effects. In detail with the sensors from P1 to P6 the side A has been checked, while with the sensors from P7 to P12 the side B has been monitored. The setup for the dynamic identification is the same of the compressive test with the steel plate at the both ends and neoprene layers positioned between the masonry specimen and the steel plates.

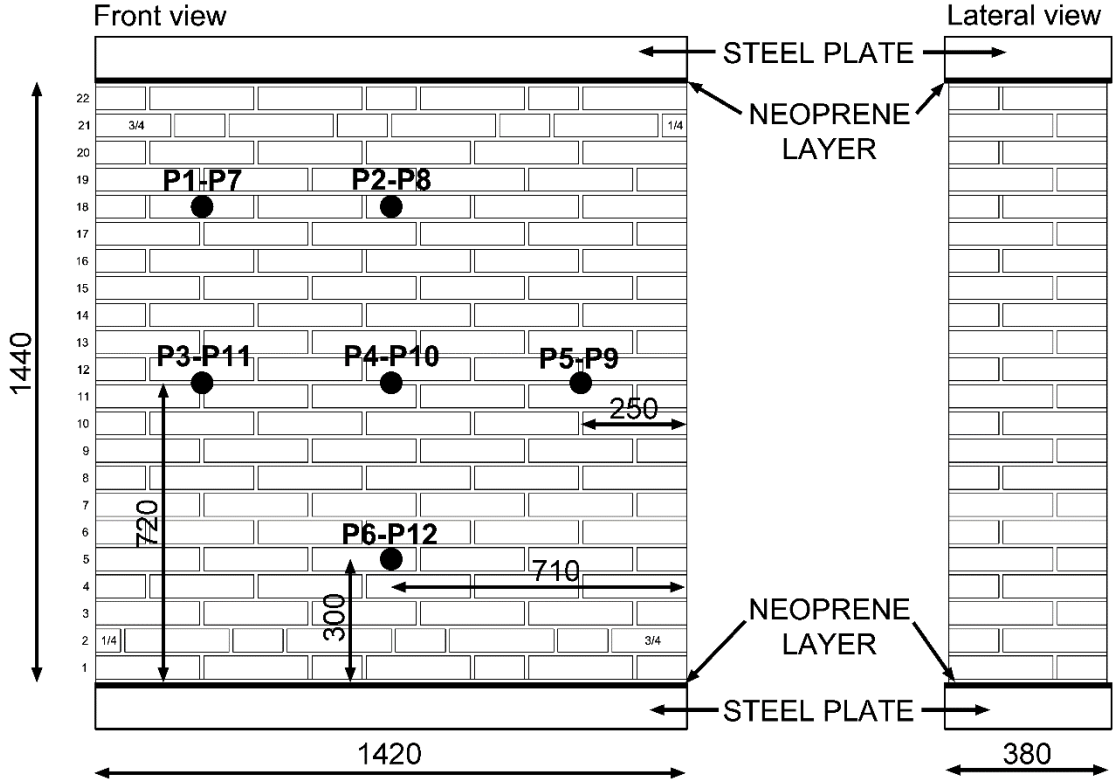

Fig. 3. Test setup and distribution of acquisition channels

3. ACQUISITION DATA AND DYNAMIC IDENTIFICATION

For the dynamic identification of masonry walls the vibrational data at initial conditions (no applied load) have been analyzed, see Figure 3. The masonry wall is located on a stiff steel plate, its dimensions are 1.40x0.40x0.10 m. A similar steel plate is located at the top of the wall to guarantee the uniform distribution of compressive load. The interaction between the steel plates and the masonry panel is through a 1 cm layer of neoprene to avoid the surface imperfections that could be influence the test.

The experimental setup was designed to investigate the global dynamic behaviour of the masonry panels. The test setup, as presented in Figure 4, was constituted by twelve uniaxial

piezoelectric accelerometers (PCB Piezotronics type 393C) with a nominal sensitivity of about 1 V/g, and a measurement range of ±2.5 g peak; the frequency range (±5%) is 0.025 to 800 Hz while the broadband resolution (1 to 10000 Hz) is 0.0001 g rms. The data acquisition system is the HBM MX840A amplifiers with 28 channels, a resolution of 24 bit and a maximum frequency range of 19.2 KHz. The accelerometers were placed on both sides to check the out-of-plan directions (Z direction, see Figure 6). The accelerometer sensors are indicated by red point and labeled by P1, P2,…Pn, Figure 6.

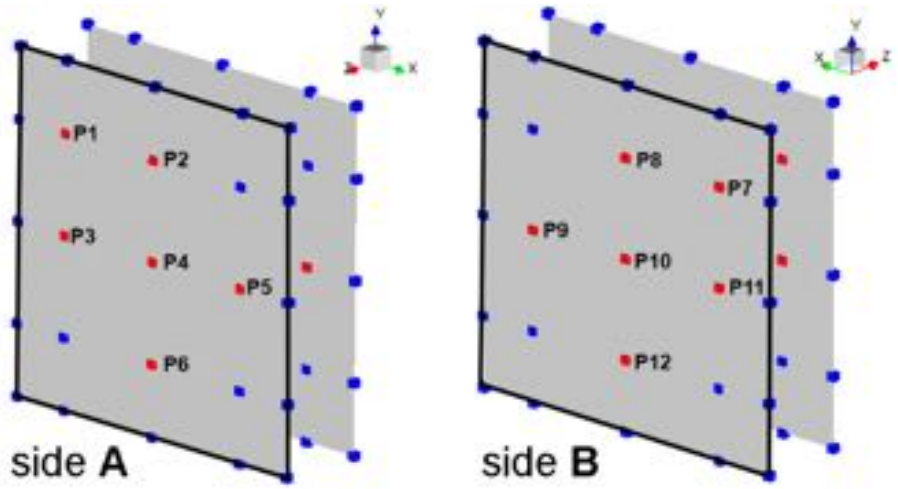

Figure 4. Configuration of accelerometers for both sides.

The accelerometers were installed by means of special metal bases fixed directly on the wall with expansion anchors in order to assure the anchorage and the stability of signal during the test above all with the starting of damaging phase. All channels were acquired with a sampling frequency of 600 Hz, for an average signal length of 1800 seconds. The signal were processed by the 4th ButterWorth filter and with a cutoff band-pass filtering of 0.25Hz-40Hz. In this paper only the first 400 seconds were analyzed in order to avoid the damage effects on dynamic parameters. Despite the dynamic response of masonry walls has been recorded with only ambient vibration every accelerogram is characterized by alternate noise and transient signal, Figure 7. The transient part is due to the unknown external excitation triggered by other testing machines.

The acquisition of the signals of the different masonry panels was conducted in similar environmental conditions, with a temperature of about 20º C and 40% of humidity.

For ambient vibration measurements with unknown input the implementation of the frequency-domain Linear Least squares estimators is proposed. The method is based on the application of a fast-stabilizing frequency domain parameter estimation through the Least Squares Complex Frequency (LSCF) estimator [22].

In detail for each recording, the cross-power spectrum function was determined in the domain of frequency, with reference to a number of measurement points. A modes extraction method based on the series of data that represent the only system's response was applied on the sole input of the ambient vibration [26]. The main vibration modes were thus identified by the best match with the compared cross-spectrum functions previously yielded from the time histories of each channel. The stabilization diagrams are obtained for some of the signals made available by dynamic monitoring. The identification procedure entails a series of pre-processing operations on the signals (mean removal, de-trending, filtering). For a detailed discussion on the identification process for masonry structures one can refer to Ceravolo [18]. The stabilization diagram is considered the most common tool to select the physical poles. In this diagram the resonance frequency and the respective damping ratio of the identified poles is visualized for different model orders.

The modal shapes have been extracted from the experimental measurements of the acceleration and consequently a 3D geometric schematic model was constructed with the commercial software [LMS Test.Lab: Siemens PLM Software, http://www.lmsintl.com]. To validate the extracted modes the modal assurance criterion, MAC [27], has been calculated between the results of every side, A and B, recorded for every masonry panel. The function of the MAC is to provide a measure of consistency between estimates of a one modal and another reference modal vector. The MAC takes on values from zero – representing no consistent correspondence, to one – representing a consistent correspondence.

For the independent check of the modal parameter estimation the frequency and damping difference are taken into account as reported in Tables 1, 2 and 3. The stability of the modes and related dynamic parameters are defined by the following limits:

- the frequency assessment is stable when the variation is less or equal to 1%;
- the variation of damping ratio must not be greater than 1%;
- the modal shape analyzed through the MAC should be at least 90% [27]; in detail the values in excess of 90% should be attained for well-correlated modes while the values of less than 10% for uncorrelated modes.

The gray boxes of Tables 1, 2 and 3 highlight the overcoming of the aforementioned limits; these values indicate the structural fault, the intrinsic damage or the manufacturing imperfection.

Starting from the better correlation between the dynamic parameters of Side A and B reported in Tables 3, 4 and 5 the flexural and torsional modal shapes, the frequencies and the related damping ratios have been determined. Figure 5 shows the typical modal shapes that have occurred on the masonry walls; the flexural (first and second) and torsional modal shapes have been

identified. The complex structure of multi-leaf masonry walls trigger uncoupled and local modal shapes. In detail the Figures 6, 8 and 9 concern the full (B1), damaged (B2) and consolidated (B3) infill masonry walls respectively.

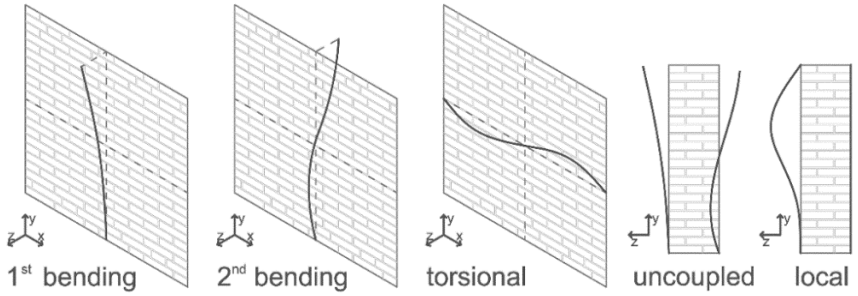

Figure 5. Typical modal shapes

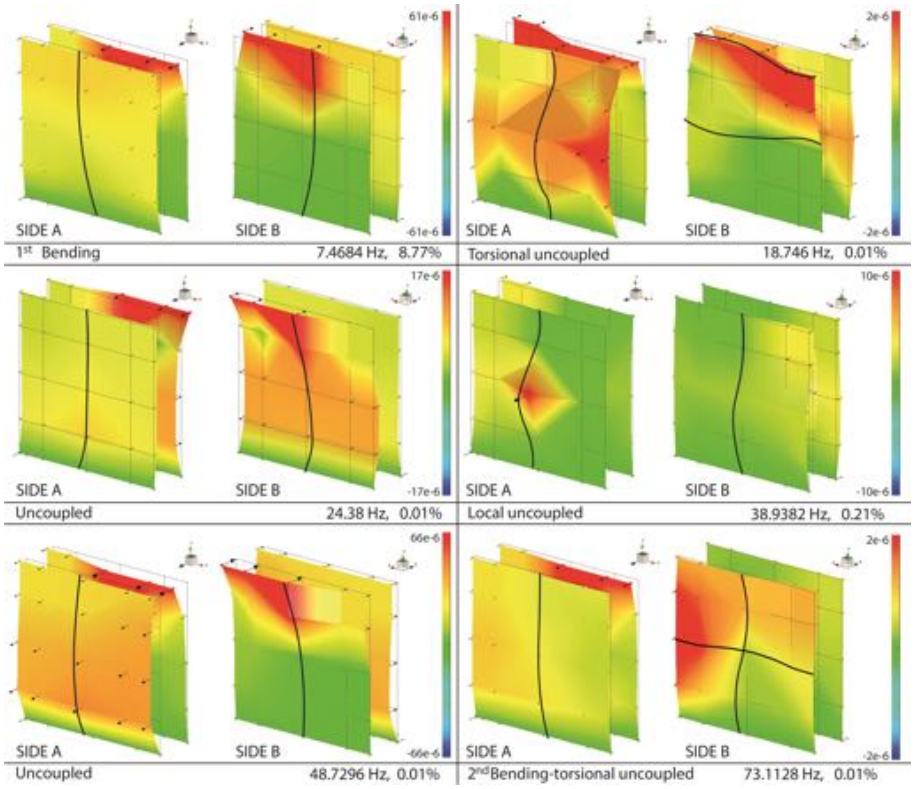

Figure 6a. Modal shapes of full infill masonry wall, B1-1

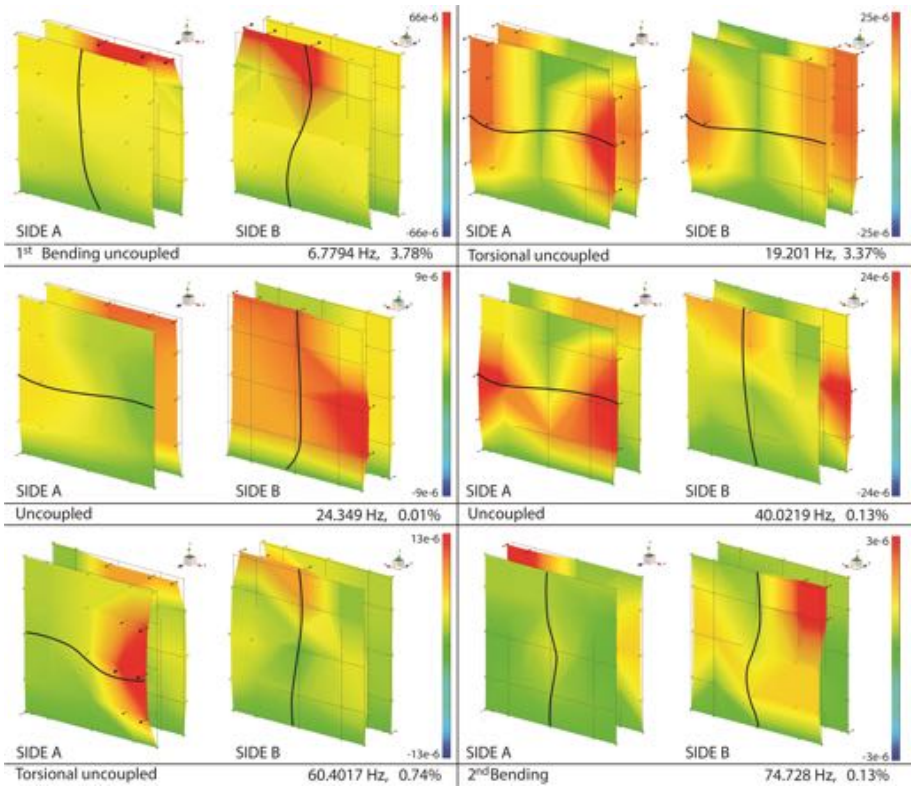

Figure 6b. Modal shapes of full infill masonry wall, B1-2

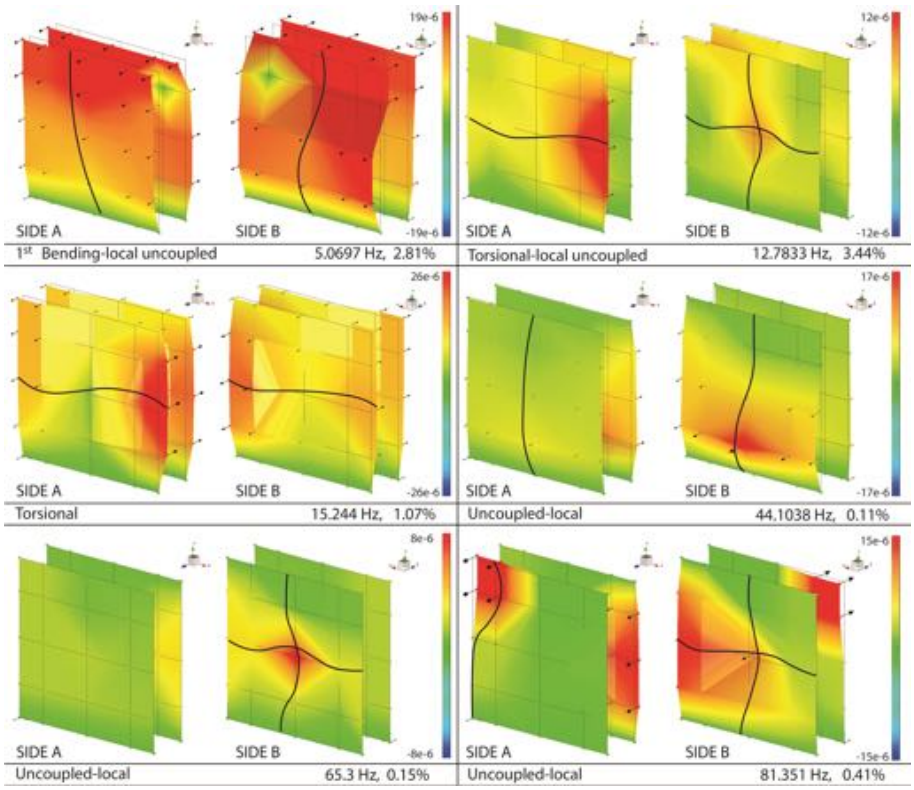

Figure 6b. Modal shapes of full infill masonry wall, B1-3

The trend of the dynamic parameters, frequencies and damping ratios, for every modal shape of typology B1 have been reported in Figures 7. For every mode of vibration the dynamic

parameters have been identified for both side, A and B. The differences between both sides are calculated in Table 1.

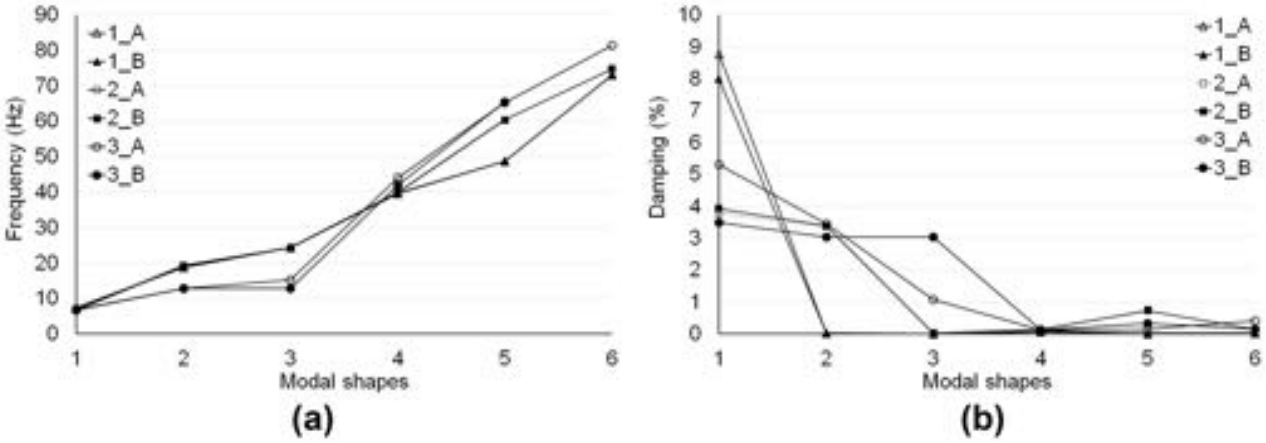

Figure 7. Dynamic parameters, (a) frequency and (b) damping ratio, for every modal shapes of B1

As shown in Figure 7 a and b the specimen with a greater incoherence between side A and B is the masonry panel B1-3. The maximum difference between the both sides has been identified with the torsional modal shape. Table 1 compares the differences of frequency and damping ratio between the both sides of every specimen of typology B1, in addition the MAC value assets the correlation between the modal vectors of side A respect to side B.

As shown in Figure 7 the Table 1 highlights and quantifies how B1-3 is characterized by uncoupled response between side A and B. In detail many frequency and damping differences are greater than 0.1 and 0.2 respectively, while some MAC values are less than 90%. For comparison the mean values for B1-1 and B1-2 specimens are 0.0175 and 0.086 of frequency and damping difference respectively; the MAC values are greater than 90%.

Mode	B1-1			B1-2			B1-3		
	Freq. Diff. (Hz)	Damp. Diff. (%)	MAC (%)	Freq. Diff. (Hz)	Damp. Diff. (%)	MAC (%)	Freq. Diff. (Hz)	Damp. Diff. (%)	MAC (%)
1	0.026	0.773	93.45	0.01	0.153	99.81	0.258	1.817	99.73
2	0.004	0	94.69	0.09	0.01	95.50	0.08	0.399	86.53
3	0.002	0.001	99.14	0.001	0.012	95.54	2.38	1.976	71.93
4	0.016	0.035	96.12	0.004	0.007	99.25	2.027	0.002	88.70
5	0.019	0.01	99.24	0.002	0.014	93.08	0.095	0.177	97.88
6	0.008	0.018	93.99	0.028	0.003	85.99	6.596	0.276	86.17

Table 1. Frequency difference, damping difference and MAC of B1 (gray boxes highlight the values out of limit, Freq. Diff. ≥1, Damp. Freq. ≥1, MAC≤90%)

Figure 8 lists the dynamic identified for B2 damaged typology.

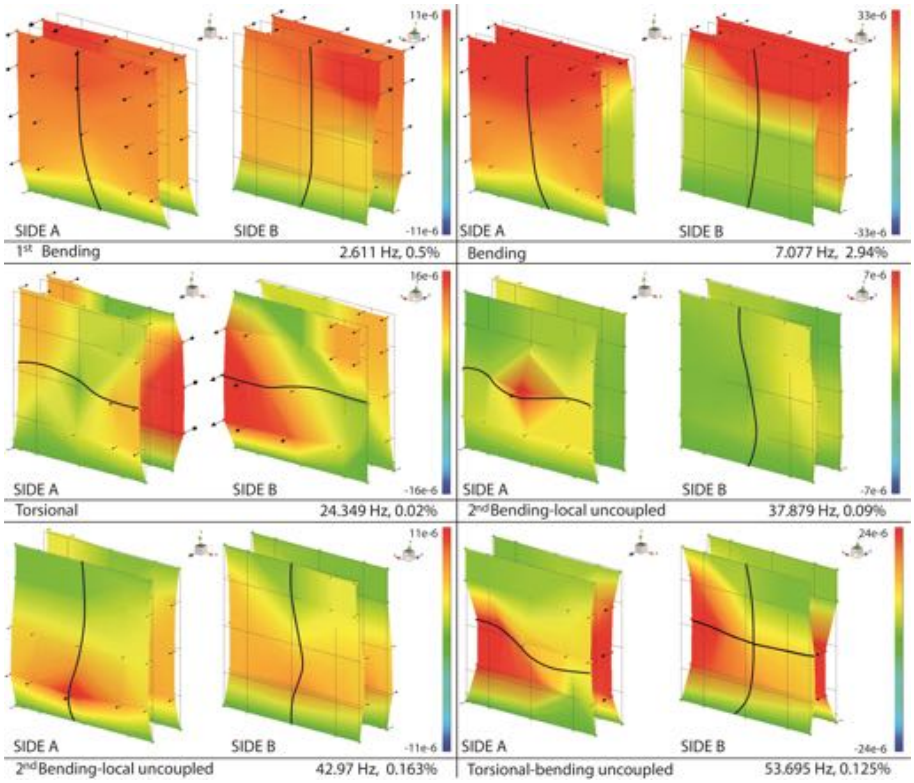

Figure 8a. Modal shapes of damaged infill masonry wall, B2-1

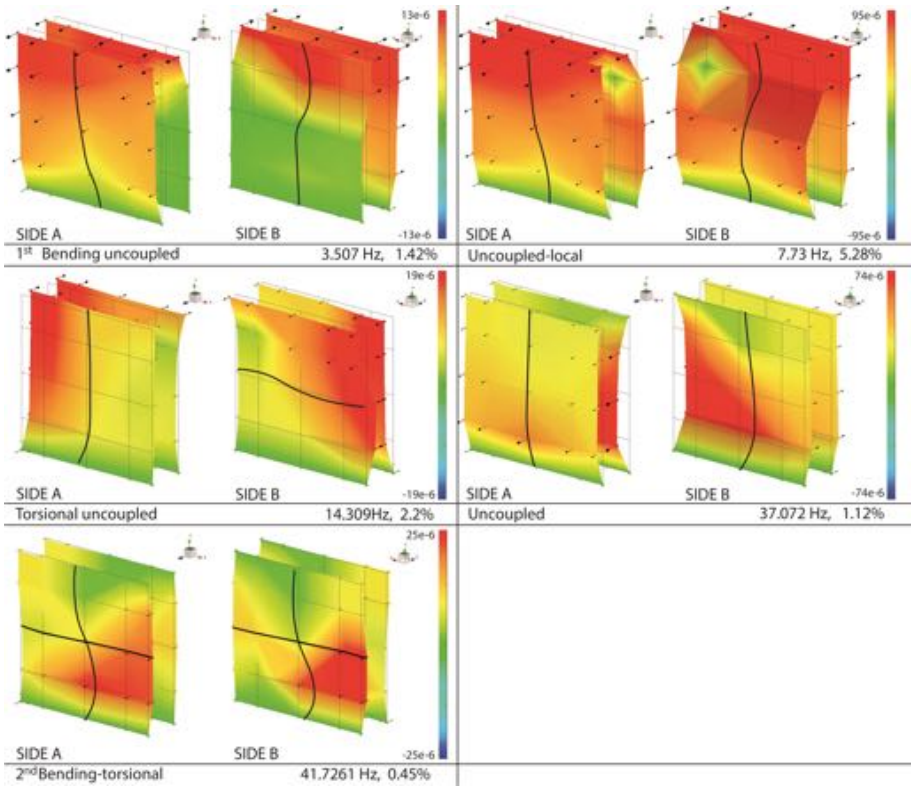

Figure 8b. Modal shapes of damaged infill masonry wall, B2-2

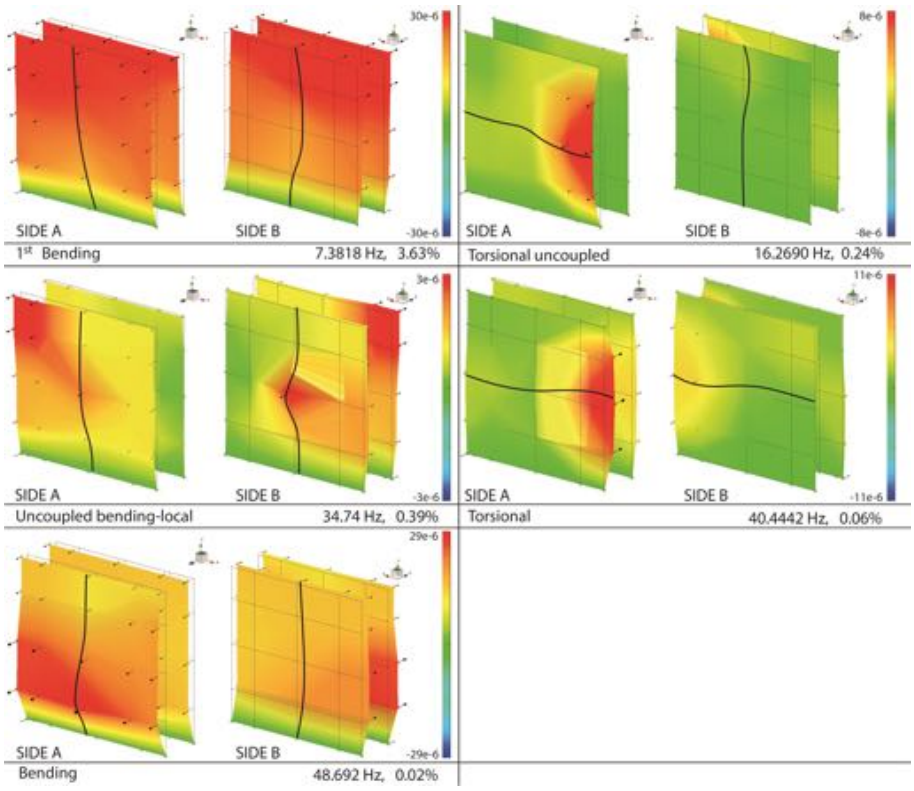

Figure 8c. Modal shapes of damaged infill masonry wall, B2-3

The comparison between the behaviour of damaged masonry walls, B2, for the different modal shapes is given by the curves reported in Figure 9. Respect to the infill masonry walls the frequency values decrease by 50%, also the trend of the damping ratios is lower than B1 typology. The analysis of correlation between the side A and B shows that only for the torsional mode of B2-3 masonry wall the two parts are completely uncoupled.

As for the B1 typology, but in a more amplified way, the torsional modal shape shows a greater difference between the masonry walls of the same typology. In detail the high slenderness and total independence between the two external leafs in relation to the geometry of the masonry walls of the damaged type mainly affect the torsional mode. As regards the dissipative capacity, the B2-3 wall has the same tendency as the infill masonry walls. B2-1 and B2-2 have high damping ratios in the second modal shape; in the first case, the lack of cohesion between the three layers of B2-1 (Figure 8a) and the identified local mode of the second wall B2-2 (Figure 8b) increase the deformation capacity.

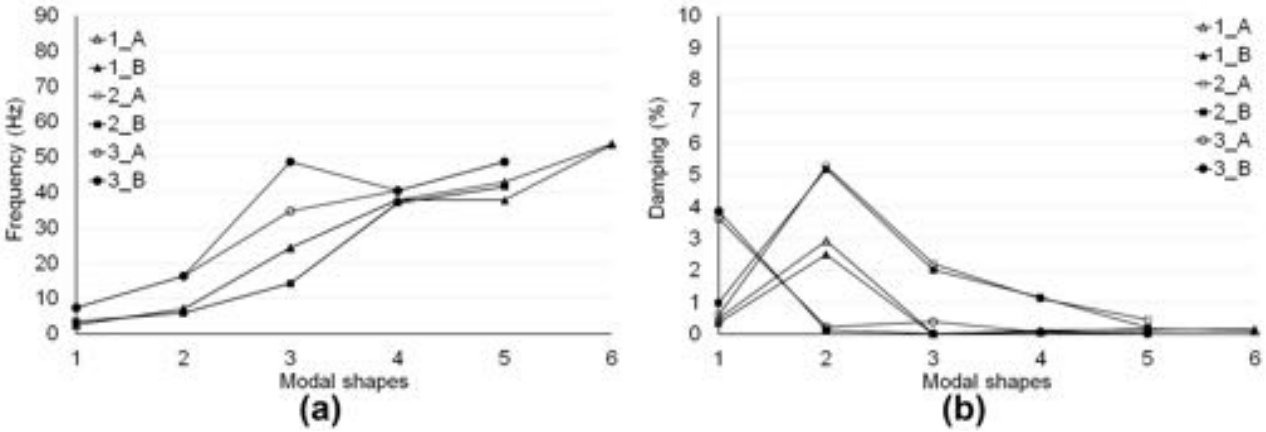

Figure 9. Dynamic parameters, (a) frequency and (b) damping ratio, for every modal shapes of B2

From the point of view of the correlation between the modal vectors of sides A and B, the MAC, with values over 90%, points out that the two leafs of the B2-1 and B2-3 masonry walls respond coherently to each other. For panel B2-1 only the first three modes of vibration recorded a MAC greater than 90% by clearly identifying the bending modes out of the plane and the torsional one; the uncoupling of the two following modes (Figure 8a) is highlighted, in addition to the low MAC value, also by the high difference between the frequency values identified, mainly due to the local modal shapes. Overall, the differences calculated for the damping ratio show that the damaged masonry walls are not affected by this parameter; the slenderness of the uncoupled masonry walls determines the deformability that remains constant and independent from the global and local responses.

Mode	B2-1			B2-2			B2-3		
	Freq. Diff. (Hz)	Damp. Diff. (%)	MAC (%)	Freq. Diff. (Hz)	Damp. Diff. (%)	MAC (%)	Freq. Diff. (Hz)	Damp. Diff. (%)	MAC (%)
1	0.002	0.139	98.873	0.006	0.392	98.987	0.006	0.226	99.924
2	0.01	0.435	99.93	0.03	0.513	99.871	0.006	0.108	92.228
3	0.009	0.016	99.314	0.058	0.194	98.496	13.95	0.365	83.928
4	0.036	0.028	72.043	0.157	0.04	95.275	0.026	0.008	93.289
5	5.055	0.047	81.428	0.02	0.241	94.69	0.002	0.005	99.787
6	0.165	0.059	84.512	0.006	0.392	98.987	0.006	0.226	99.924

Table 2. Frequency difference, damping difference and MAC of B2 (gray boxes highlight the values out of limit, Freq. Diff. ≥1, Damp. Freq. ≥1, MAC≤90%)

Figure 10 lists the dynamic identified for B3 consolidated infill masonry walls typology.

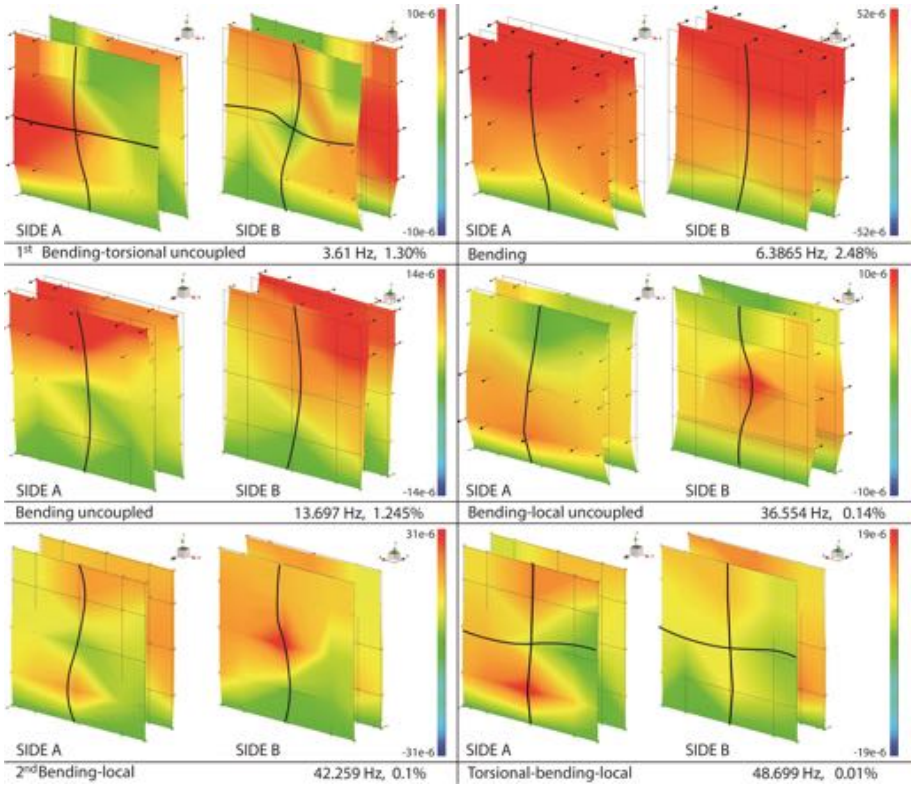

Figure 10a. Modal shapes of consolidated infill masonry wall, B3-1

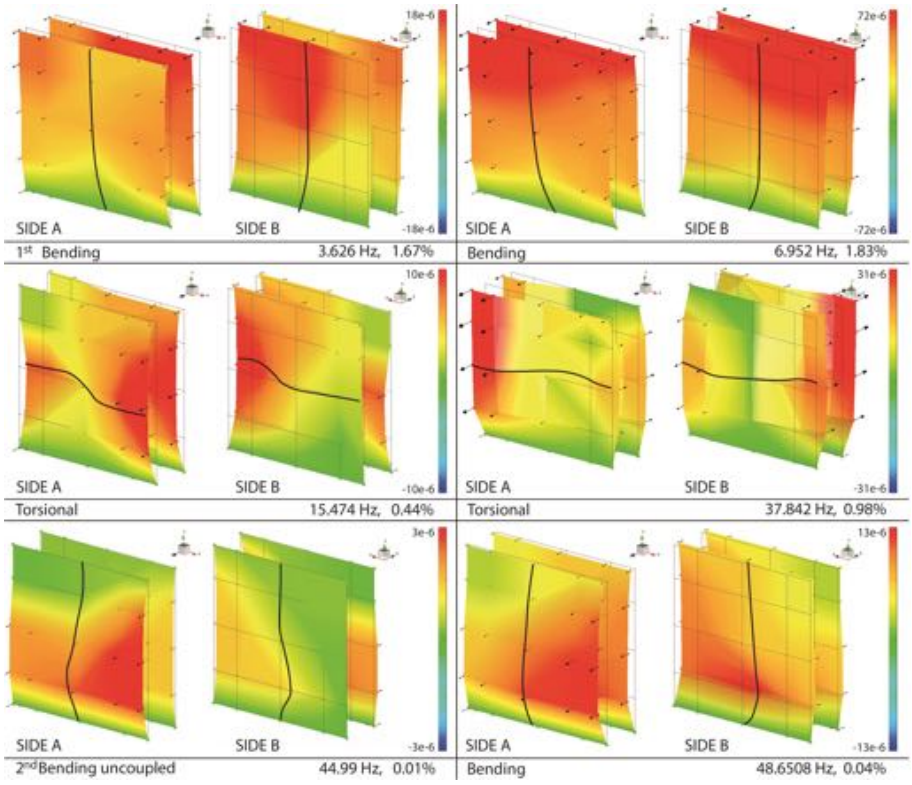

Figure 10b. Modal shapes of consolidated infill masonry wall, B3-2

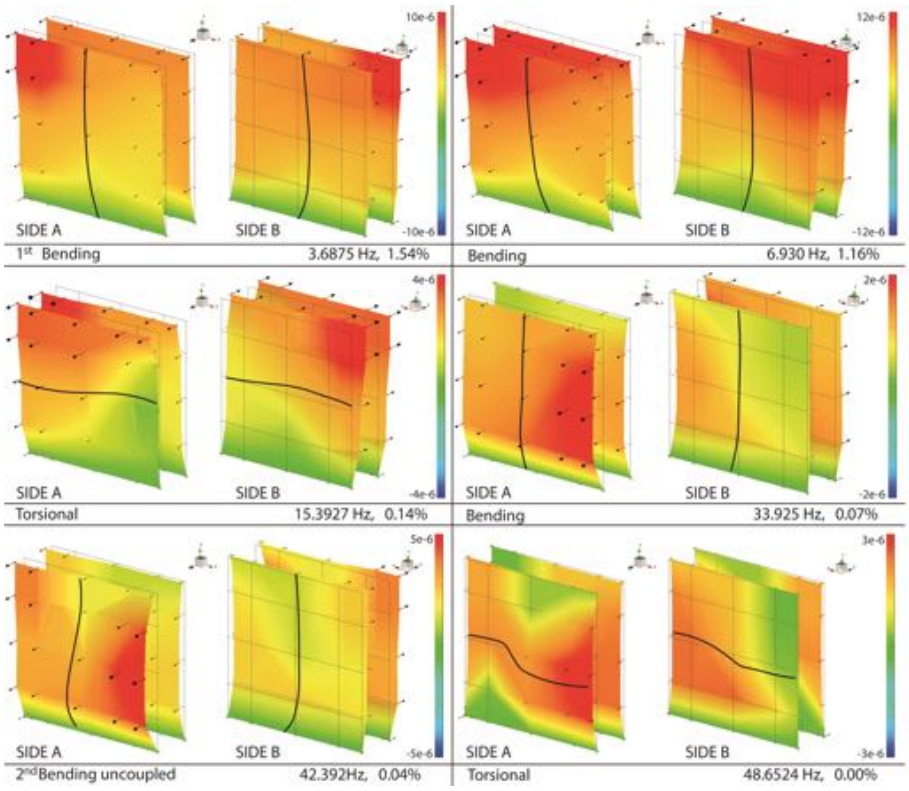

Figure 10c. Modal shapes of consolidated infill masonry wall, B3-3

The effect of the consolidation intervention for the B3 masonry walls is evident from the homogeneous response between the walls of the same panel and between the panels themselves for the identified dynamic parameters, frequencies (Figure 11a) and damping ratios (Figure 11b). As for the frequencies identified, the values are similar to panels of type B2; only the B3-1 masonry wall, which for the modal shapes 4 and 5 is characterized by local modes (see Figure 10a), has identified lower frequency values than the overall trend. Damping ratios (Figure 11b) confirm what it's said for the frequencies as they show in every modal shape a global response of the masonry wall and a good compliance between the three panels. The tendency of the damping ratios decreases steadily with values less than 40% compared to the trend of the B2 type panels.

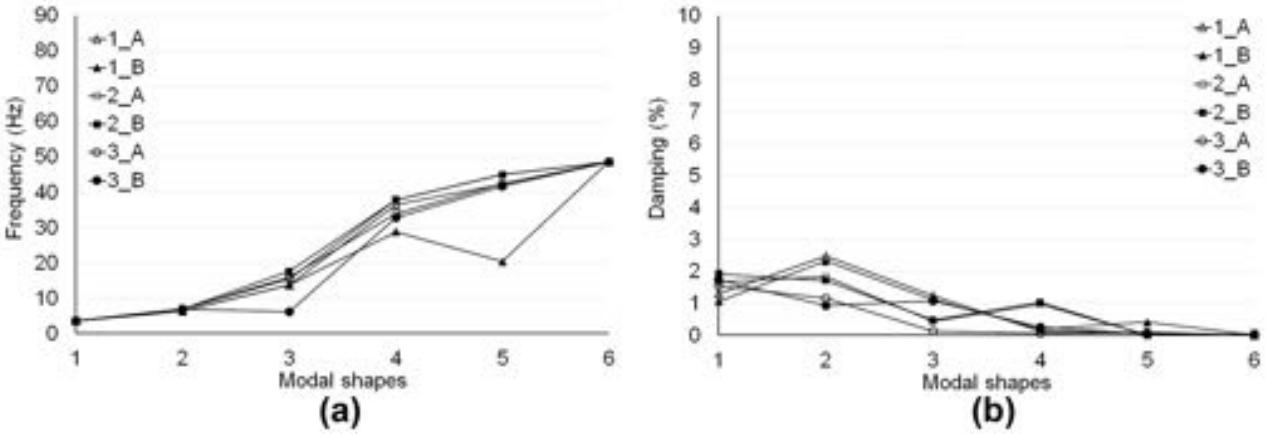

Figure 11. Dynamic parameters, (a) frequency and (b) damping ratio, for every modal shapes of B3

Table 3 shows that for the modal shapes 4 to 6, the response of masonry wall B3-1 is conditioned by local modes; in detail the MAC values are less than 75% while the difference between the frequencies is greater than 7 Hz. The masonry wall B3-2 highlights through the different stiffness between the two sides A and B, with a difference between the frequencies of about 2 Hz and with the MAC less than 56%, which only the torsional mode is conditioned by an uncoupling between the external leafs. Also for the B3-3 wall, the torsional mode highlights a difference in frequency between the two sides A and B although the relationship between the modal vectors is in very good agreement with a MAC greater than 90%.

Mode	B3-1			B3-2			B3-3		
	Freq. Diff. (Hz)	Damp. Diff. (%)	MAC (%)	Freq. Diff. (Hz)	Damp. Diff. (%)	MAC (%)	Freq. Diff. (Hz)	Damp. Diff. (%)	MAC (%)
1	0.009	0.241	96.132	0.013	0.256	99.24	0.012	0.197	99.03
2	0.003	0.152	99.97	0.003	0.11	99.987	0.012	0.212	99.353
3	0.022	0.117	98.802	2.168	0.034	55.325	9.705	0.949	92.801
4	7.759	0.052	70.713	0.075	0.051	89.902	1.019	0.179	57.638
5	21.821	0.311	22.405	0.001	0.004	99.891	0.665	0.059	75.283
6	0.008	0.003	51.362	0.003	0.009	99.916	0.001	0.002	99.349

Table 3. Frequency difference, damping difference and MAC of B3 (gray boxes highlight the values out of limit, Freq. Diff. ≥1, Damp. Freq. ≥1, MAC≤90%)

4. NUMERICAL MODELS

Finite Element models of the masonry specimens tested in laboratory have been realized: a comparison between experimental and numerical results is provided. The purpose is to evaluate reliability of the models to describe the behavior of multi-leaf masonry panels and their limit of applicability. In particular attention is paid to the mechanical properties to be adopted to model masonry material and the internal infill. Mechanical properties of masonry external walls have been defined by means of homogenization procedure, adopting for the material components at micro-scale the mechanical properties obtained by the mechanical characterization in lab. Then, a parametric modal analysis varying the properties of the infill has been performed, in order to calibrate the model of the whole panel: external walls and internal fill. The comparison between numerical and experimental natural frequencies allows identifying the mechanical properties. In order to verify the reliability of the dynamic identification, non-linear static analysis has been performed to reproduce the compressive test performed in lab, allowing identifying the appropriate mechanical parameters.

The difficulties in modeling masonry are related to its composite nature, to the size of heterogeneity, to geometric complexities and to the presence of the infill. The literature regarding models and analyses of masonry structures is wide. Many different approaches may be found, among which the most common strategies adopted are the use of discrete or continuous models [28, 29, 30, 31, 32, 33, 34].

In this work, continuous models are proposed. A multi-scale periodic homogenization procedure is adopted [24] to define an equivalent continuum able to reproduce at the macro-scale the characteristics of masonry emerging at the micro-scale. The procedure consists of the solution at micro-scale of a field problem by applying on a representative element of volume (REV) cinematic periodic boundary conditions. The REV provides all the mechanical and geometrical characteristic of masonry needed to completely describe the whole panel, which is generated by its repetition. The solution of the field problem on the REV provides the macroscopic mechanical properties to be adopted at the macro-scale. Here a full 3D procedure of homogenization [25] has been adopted. Equivalent orthotropic continuum is adopted for the external masonry walls, while the infill has been modeled as an isotropic continuum with mechanical properties reduced with respect to masonry walls. Geometrical description of REV and boundary conditions applied are reported in Fig. 12. Mechanical properties adopted in FEM models for external masonry walls are reported in Table 4. For upper and lower brick layers, an increase of 50% of mechanical properties has been assumed, in order to take into account the presence of cement mortar reinforced by steel textile.

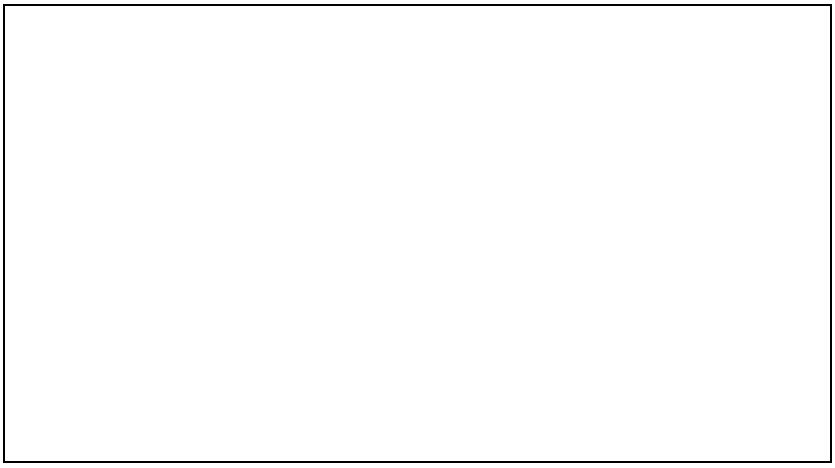

Fig. 12. Representative Element of Volume (REV) and periodic boundary conditions applied.

Table 4. Mechanical properties of the FE model.

External masonry walls		
Young's Moduli [MPa]	Shear Moduli [MPa]	Poisson's Coefficients
$E_{11} = 3450$	$G_{12} = 765$	$\nu_{12} = 0.220$
$E_{22} = 3063$	$G_{23} = 782$	$\nu_{23} = 0.248$
$E_{33} = 3560$	$G_{31} = 933$	$\nu_{31} = 0.210$

Parametric natural frequencies analyses have been performed to calibrate the proposed models [35]. A series of models have been realized in order to reproduce the dynamic behavior of the different walls. The dynamic identification showed that the frequencies of full infill walls are higher than the ones of damaged infill walls. Moreover, damaged infill walls exhibit uncoupled and local modal shapes, while full infill walls exhibit global mode, typical of its monolithic behavior. Consolidated infill walls show frequencies lower with respect to full infill walls, closer to the ones of the damaged infill walls, but at the same time the injections provide a monolithic behavior, as shown by the global modes detected, and a lower dispersion in data results.

Models are realized by means of 3D bricks elements, adopting a commercial FE code [36]. Models reproduce the setup of the test: base is fixed and steel bar on top is modeled. In the case of full infill walls, the infill has been modeled as an isotropic continuum. The choice is justified by the fact that the infill has been built with brick potsherds filled with mortar (see Fig. 4): therefore the internal core can be assumed as a continuum, having a lower value of mechanical properties with respect to the ones of external walls. Varying the properties of the infill it has been possible to calibrate the model obtaining frequencies very close to the experimental ones. In particular, a

Young's modulus equal to E_{22} reduced of 10% and an higher value of Poisson's coefficient, equal to 0.4, provided results in good agreement with the experimental ones. The first mode has been adopted for the comparison. The analysis has been performed at the initial stage of the compressive test, applying 117 kN of load, the load reached after 400 seconds from the beginning of the test, equivalent to around $1/20^{th}$ of the collapse load. The model is provided in Figure 13 (a). The first 6^{th} modal shapes and the relative frequencies are reported in Figure 14.

In the case of damaged infill walls, several values of mechanical properties of infill have been analyzed. However, due to the intrinsic characteristics of continuous models, global modes are obtained, and even the adoption of very low values of mechanical properties of infill do not provide decrease of frequencies comparable with the experimental ones. Therefore a model in which the two external are assumed separated has been proposed. This choice is justified by the fact that damaged filling has been realized only with brick potsherds (see Fig. 4), therefore the external walls behave like two separated panels, obtaining frequencies closer to the experimental ones. The models is shown in Figure 13. The first 6^{th} modal shapes and the relative frequencies of the two models are reported in Figure 14 and 15.

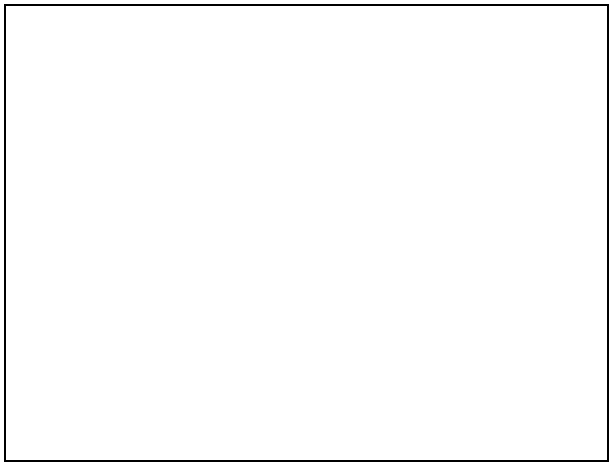

Figure 13. (a) Model of full infill; (b) Model of damaged infill

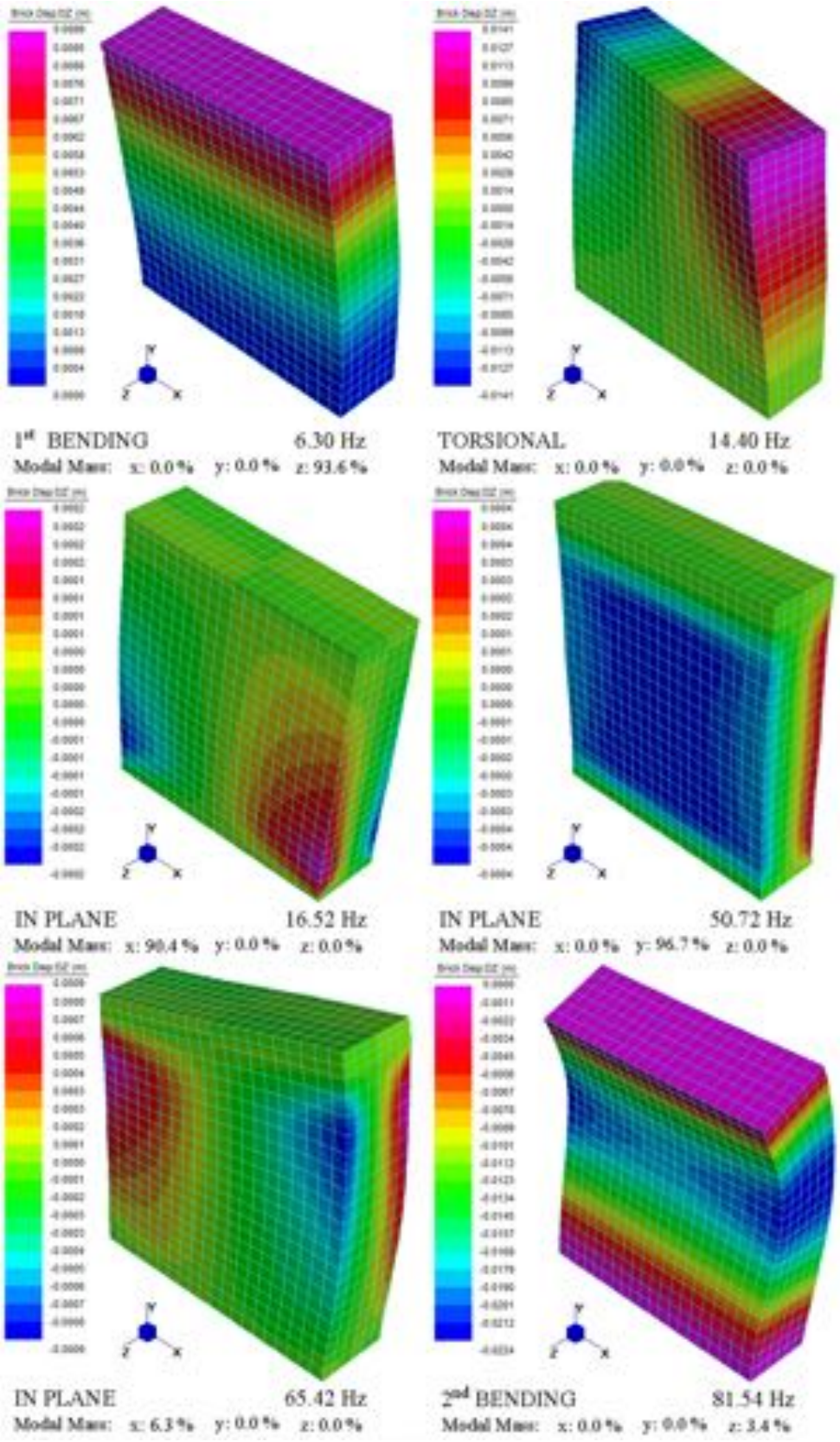

Figure 14. Modal shapes, frequencies and modal mass of full infill FEM

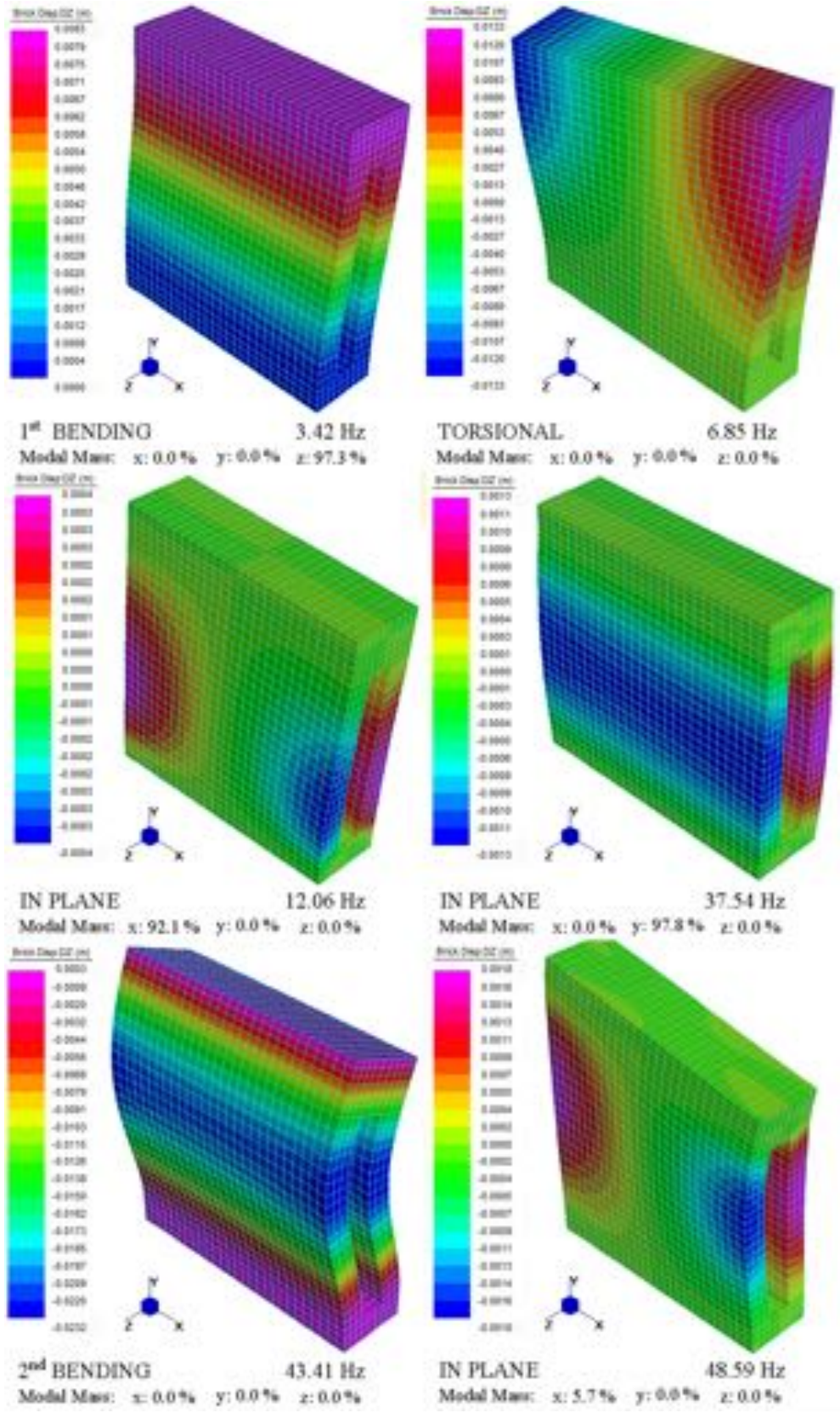

Figure 15. Modal shapes, frequencies and modal mass of damaged infill FEM

The proposed models seems to be suitable to reproduce the dynamic behavior of the full and damaged infill walls, while the improvements provided by injections in terms of frequencies are more difficult to be caught. The adoption of more appropriate models is suggested.

5. COMPARISON BETWEEN EXPERIMENTAL AND NUMERICAL DYNAMIC PARAMETERS

For every mode of vibration the frequency values corresponding to three masonry walls are listed; the mean value and the standard deviation SD of every typology are calculated in order to highlight the dispersion of results and the differences between the same typology due to imperfection and/or intrinsic characteristics. The difference between experimental and numerical results are reported in the last columns of Tables 5 and 6 through the coefficient of variation COV. Table 5 shows the comparison between experimental and numerical data of full infill masonry walls B1, while Table 6 combines the response of damaged and consolidated masonry walls, B2 and B3 respectively, because the FE analysis failed to simulate the difference between the two types.

For the first flexural mode the fundamental frequencies correspond to a greater stiffness of masonry walls that founds confirmation in the structural response to compressive test as shown in Figure 16 and in Table 5; in detail to the increment of fundamental frequency values from B1-3 to B1-1 corresponds to the increase of the maximum load reached during the compression tests (Table 9). The higher values of the standard deviation SD (greater than 1) highlights how much the manufacturing imperfections affect the response of the full infill masonry walls respect to damaged and consolidated types. The gap between the three wall panels for each vibration mode does not allow a good match with the coefficient of variation COV that remains below 10% for only a few specimens.

Mode of vibration	EXP			FEA (Hz)	$COV_{EXP-FEA}$ (%)
	(Hz)	Mean value (Hz)	SD		
Mode 1, 1st bending	7.47	6.44	1.24	6.305	15%
	6.78				7%
	5.07				20%
Mode 2, torsional	18.74	16.9	3.58	14.4	23%
	19.2				25%
	12.78				11%
Mode 3	24.38	21.32	5.27	16.52	32%
	24.35				32%
	15.24				8%
Mode 4	38.93	41.01	2.73	50.72	24%
	40.02				21%
	44.1				13%
Mode 5	48.73	58.14	8.51	65.42	25%
	60.4				7%
	65.3				0.6%
Mode 6 2nd bending	73.11	76.39	4.37	81.54	10%
	74.73				8%
	81.35				0.2%

Table 5. Comparison between experimental and numerical frequency values, full infill masonry walls B1

The comparison between experimental and numerical modal shapes of B1, B2 and B3 masonry walls have been reported in Figures 15, 16 and 17. For every masonry panel have been compared the first bending (a), the second bending (c) and the torsional (b) modal shapes through the normalized modal displacements. The modal shapes have been outlined considering the vertical and horizontal barycentric directions for both side, A and B. Considering that for the numerical model the modal shapes involve globally the masonry walls, avoiding local and uncoupled modal shapes (see Figures 14 and 15), the curves of modal shapes have been reported symmetrically respect to Y-axis for 1st and 2nd bending (FEM_vertical) and respect to X-axis for torsional (FEM_horizontal) modal shapes.

The experimental response has been labelled with A and B for both side, with vertical for the 1st and 2nd bending and with horizontal for the torsional modal shapes, obtaining A and B-vertical or A and B-horizontal.

In detail for the B1 masonry walls, the first experimental flexural mode (a) corresponds to FEM modal shapes, excluding the uncoupled mode of B1-3, which relate the first flexural mode of side A to the second flexural mode of side B. For the torsional modal shape only B1-3 highlights a

good match between the experimental and FEM modal shapes. The second bending mode (c) shows a good EXP-FEM correspondence with the masonry walls B1-2 and B1-3 as shown in Table 5 where the coefficient of variation is less than 10%.

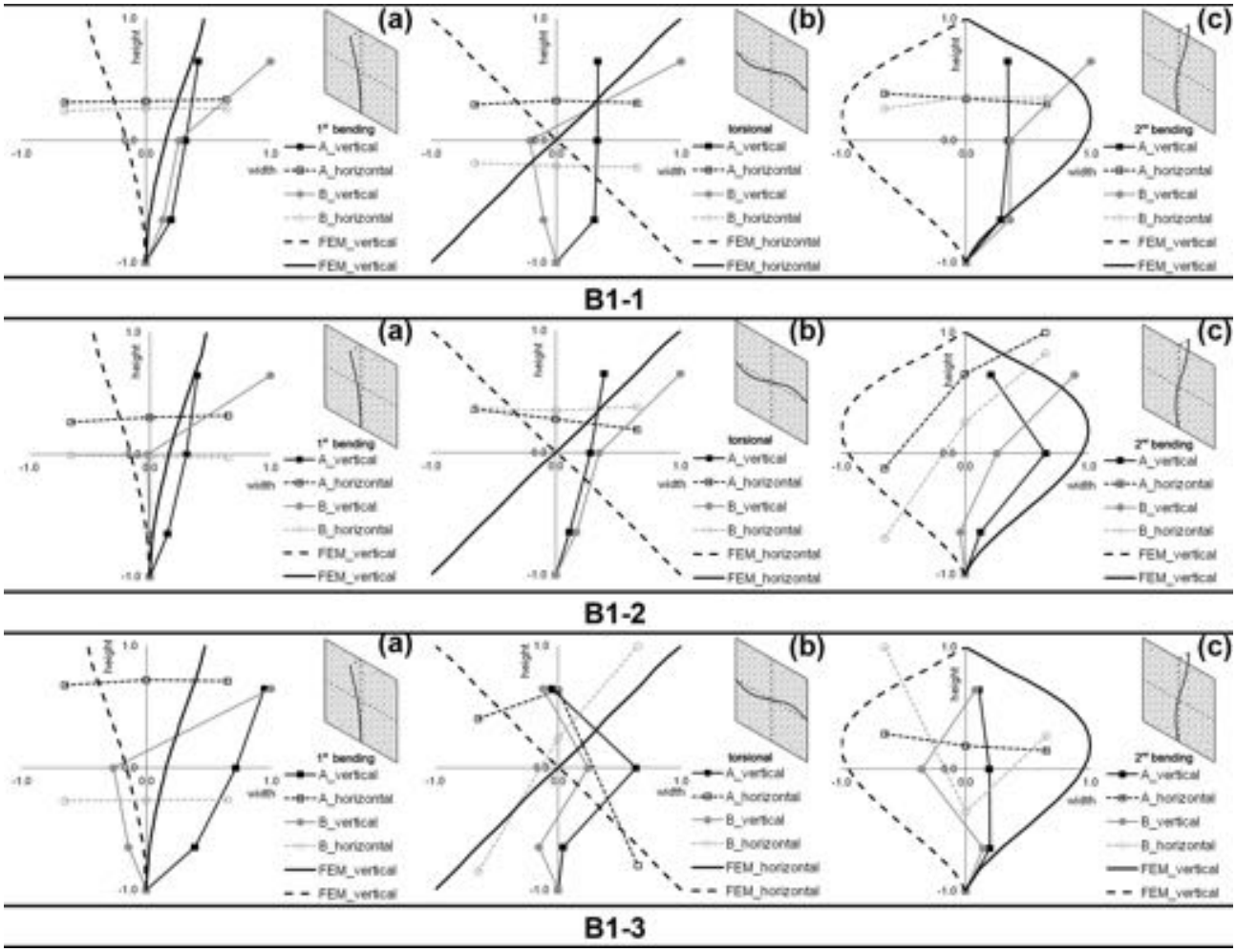

Figure 16. Experimental and numerical comparison of modal shapes, B1 masonry walls

Table 6 compares the experimental values of B2 and B3 masonry walls with the numerical results. The standard deviation SD value less than 1 shows that for some modes of vibration, identified experimentally, the difference between the masonry walls of the same typology are negligible. This aspect is confirmed by the maximum load achieved through the compressive tests recording a similar failure threshold for both typologies, B2 and B3 (see Figure 17 and Table 6).

The COV (coefficient of variation) calculated for every typology shows, with values less than 10%, a good agreement between experimental and numerical results, see Table 6.

Mode of vibration	EXP						FEA (Hz)	$COV_{EXP, B2\text{-}FEA}$ (%)	$COV_{EXP, B3\text{-}FEA}$ (%)
	B2			B3					
	(Hz)	Mean value (Hz)	SD	(Hz)	Mean value (Hz)	SD			
Mode 1, 1st bending	2.61	3.06	0.64	3.61	3.64	0.04	3.42	24%	5%
	3.51			3.62				3%	6%
	n.i.			3.68				*n.i.*	7%
Mode 2, torsional	7.07	7.39	0.33	6.38	6.75	0.32	6.85	3%	7%
	7.73			6.95				13%	1%
	7.38			6.93				8%	1%
Mode 3	24.35	18.31	5.32	13.69	14.84	1.00	12.06	50%	12%
	14.31			15.47				16%	22%
	16.26			15.37				26%	22%
Mode 4	37.88	36.56	1.63	36.55	36.10	2.00	37.54	1%	3%
	37.07			37.84				1%	1%
	34.74			33.92				8%	11%
Mode 5, 2nd bending	42.97	41.71	1.27	42.26	43.21	1.54	43.41	1%	3%
	41.72			44.99				4%	4%
	40.44			42.39				7%	2%
Mode 6	53.69	51.19	3.54	48.7	48.67	0.03	48.59	9%	0%
	n.i.			48.65				*n.i.*	0%
	48.69			48.65				0%	0%

n.i. not identified

Table 6. Comparison between experimental and numerical frequency values, damaged B2 and consolidated B3 infill masonry walls

The organization of Figures 17 and 18 is the same adopted for the Figure 16.

For all masonry walls of both types B2 and B3 the first flexural modal shape (a) shows a good correspondence between the experimental and numerical behaviour except for the B3-1 panel characterized by the second flexural mode. For torsional modal shape (b), the good correspondence between EXP and FEM is evident for B2-1 and B2-3, while for B2-2 the uncoupled flexural modes are predominant.

For the torsional mode of the B3 masonry walls only B3-2 and B3-3 show a relationship between experimental and FEM modal shapes; this correspondence is also confirmed by the coefficient of variation shown in Table 6, equal to 1% for the second and third panels, B3-2 and B3-3 respectively, and 7% for the B3-1.

The good correlation between EXP and FEM of the second flexural modal shape (c) is evident for both B2 and B3 types (see Figures 17 and 18) and it's confirmed by the COV (Table 6) with values less than 8%.

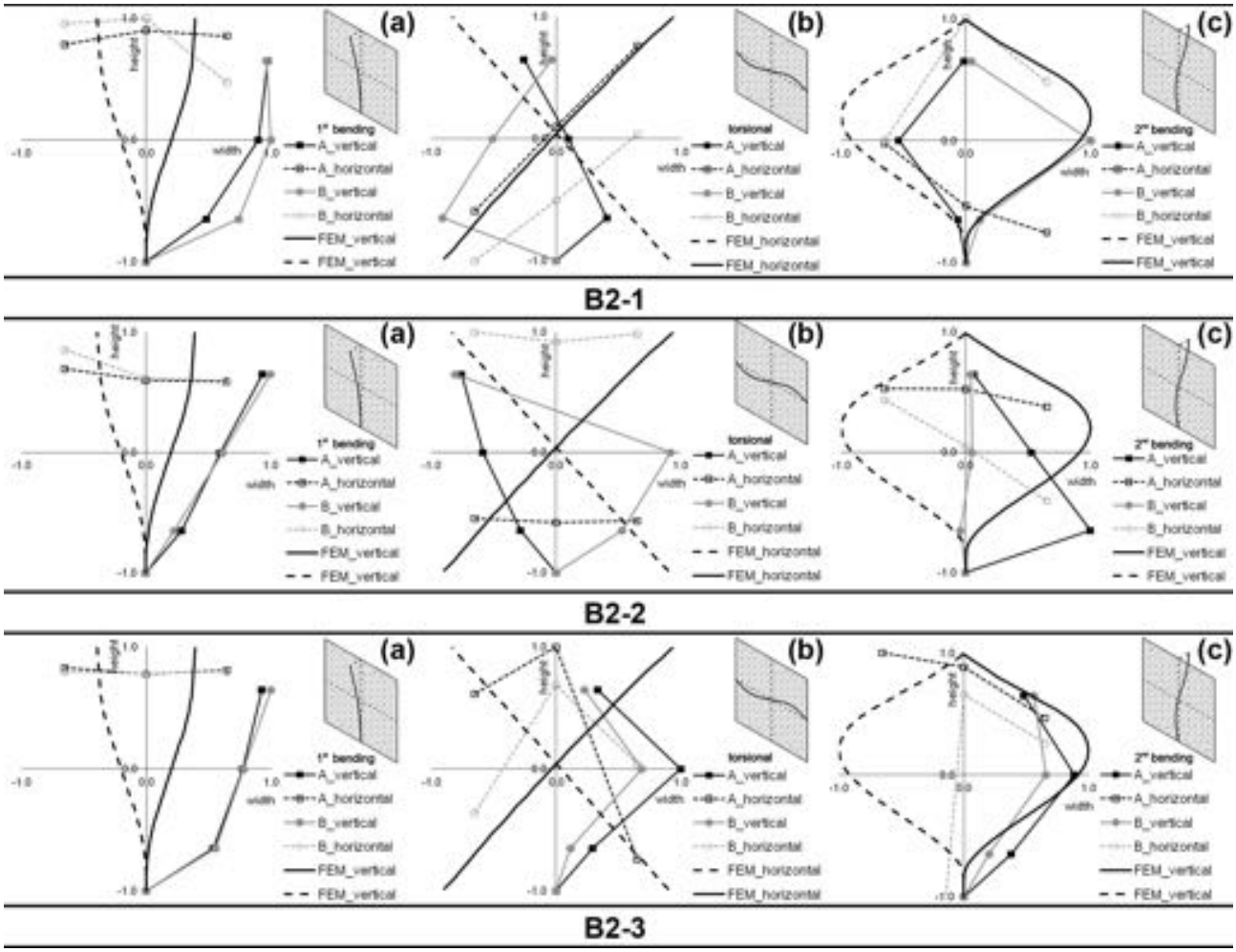

Figure 17. Experimental and numerical comparison of modal shapes, B2 masonry walls

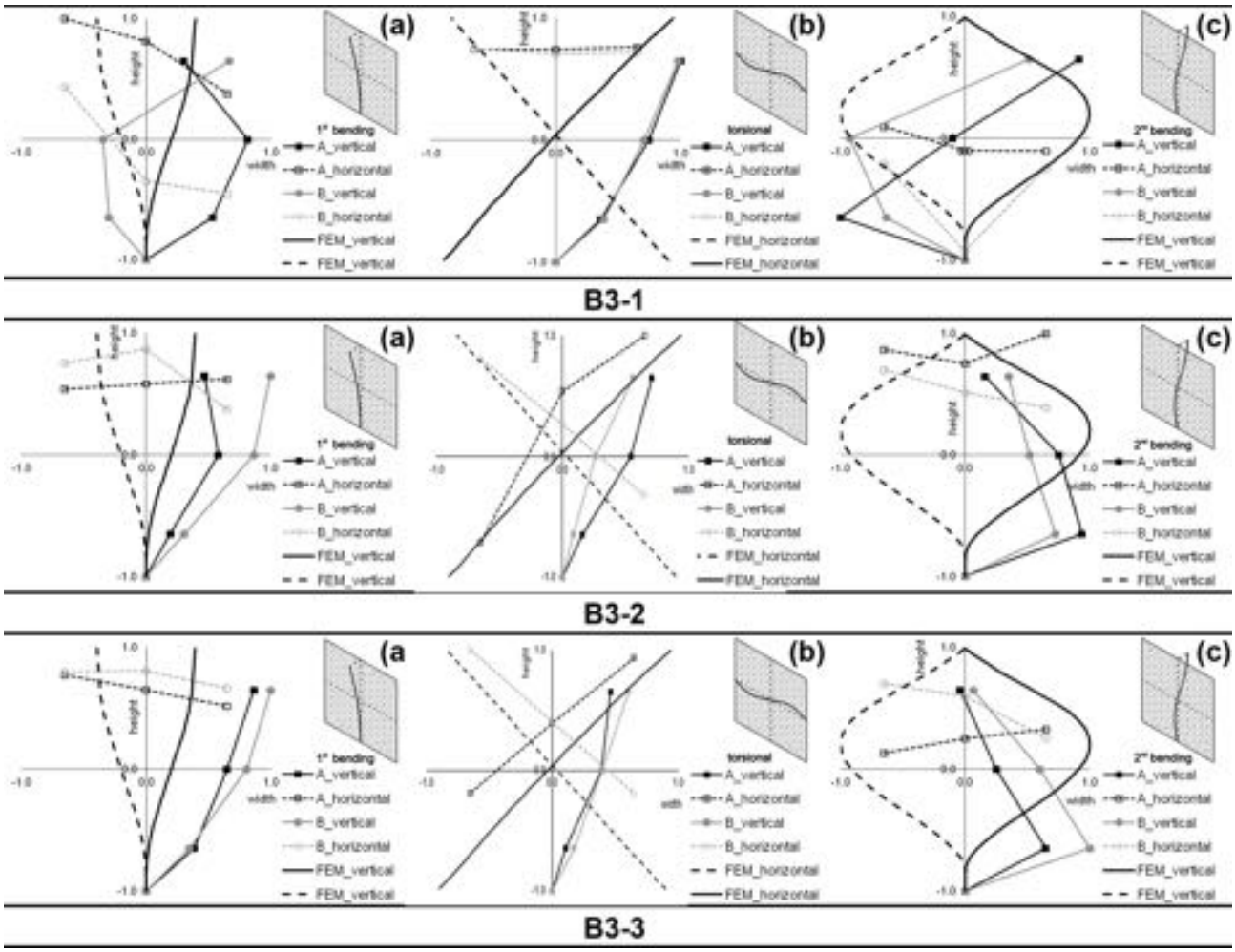

Figure 18. Experimental and numerical comparison of modal shapes, B3 masonry walls

CONCLUSIONS

Based on the numerical and experimental results the following considerations can be drawn:

- the dynamic parameters allow a first prediction about the structural response of the multi-leaf masonry walls characterized by a complex structure;
- of the three dynamic parameters that characterize the wall panels, only the modal shapes and the related frequencies allow to experimentally identify uncoupled modal shapes. The damping ratio only ensures the identification of local modal shapes;
- the adopted approach based on multi-scale periodic homogenization procedure, on mechanical characterization of material constituents and on global dynamic identification allows to simulate the complex structure of three-leaf masonry walls with appreciable agreement;
- the infill masonry walls show a greater uncertainty between the experimental dynamic parameters and a bigger difference between the experimental and numerical results than

other typologies. The manufacturing imperfection, the heterogeneity and the intrinsic characteristics affect most the infill masonry walls B1 showing their structural complexity than other masonry walls, B2 and B3;

- comparing the experimental and numerical results the first bending modal shapes of all masonry walls - B1, B2 and B3 - correspond with good agreement, while the frequencies vary with a coefficient of variation greater for B1 than B2 and B3;
- the torsional modal shape is difficult to identify in the infill masonry walls (B1) while it is easy to outline in damaged (B2) and consolidated (B3) typologies. The strength structural frame and the slender panel of type B2 and B3 are easier to activate the torsional mode while the infill masonry wall responds globally, predominantly with bending mechanisms out of the plane. Compared to the frequencies identified, the experimental and numerical comparison finds the best correlation between the results in types B2 and B3 than B1;
- the second bending modal shapes are experimentally identified with good approximation for all masonry walls. Altogether, also modal parameters calculated with the FE model are in good agreement with the experimental results;
- the contribute offered by consolidating intervention not allow an increment of strength. The improvement regards the quality of the masonry walls in terms of the better homogeneity and continuity as shown by lower standard deviation values of consolidated infill typology than others;
- the homogeneity of B3 masonry walls, assured by consolidating intervention, guarantees the best agreement between the experimental and numerical results;
- the size effects influence the global response of three-leaf masonry walls that not pay the differences of damaged or consolidating typologies. After the first bending modal shape the uncoupled responses characterize the dynamic behaviour of every leaf, that are affected by the absence of the transversal links between leafs and by the potential out-of-plan failure mechanism triggered by the slenderness of every leaf.
- for every masonry wall the size effect triggers a frame strength mechanism that affects the dynamic behaviour of infill panels constituted by both external leafs. This mechanism affects the failure mode of every masonry wall;

Next step of this research is the adoption of the models to investigate the compressive tests, in order to investigate the behaviour of multi-leaf masonry walls. Moreover, dynamic measure collected during the compressive tests will be analysed: the purpose is to evaluate how dynamic parameters vary at increasing of the damage due to the compressive load applied.

Acknowledgments

The research has been carried out thanks to the financial support of PRIN 2015 (under grant 2015JW9NJT_014, project "Advanced mechanical modeling of new materials and structures for the solution of 2020 Horizon challenges").

The tests were carried on at the Laboratory of Strength of Materials (LabSCo) of IUAV University of Venice; the author warmly thanks the technical staff of LabSCo for the collaboration and support during the tests.

REFERENCES

[1] Binda, L.; Baronio, G.; Penazzi, D.; Palma, M. & Tiraboschi, C. (1999), Caratterizzazione di murature in pietra in zona sismica: DATA-BASE sulle sezione murarie e indagini sui materiali, *in* 9° Convegno Nazionale «L'ingegneria sismica in Italia».

[2] Binda, L.; Pina-Henriques, J.; Anzani, A.; Fontana, A. & Lourenço, P. B. (2006), A contribution for the understanding of load-transfer mechanisms in multi-leaf masonry walls: Testing and modelling, *Engineering Structures* **28**(8), 1132-1148.

[3] Ramalho, M. A.; Taliercio, A.; Anzani, A.; Binda, L. & Papa, E. (2008), A numerical model for the description of the nonlinear behaviour of multi-leaf masonry walls, *Advances in Engineering Software* **39**(4), 249-257.

[4] Ramalho, M.; Papa, E.; Taliercio, A. & Binda, L. (2005), A numerical model for multi-leaf stone masonry, *in* '11th International Conference on Fracture 2005, ICF11', pp. 3247-3252.

[5] Ramalho, M.; Taliercio, A.; Anzani, A.; Binda, L. & Papa, E. (2005), Experimental and numerical study of multi-leaf masonry walls, *in* 'WIT Transactions on the Built Environment', pp. 333-342.

[6] Oliveira, DV; Silva, R.A.; Garbin, E.; Lourenço, P.B. (2012) Strengthening of three-leaf stone masonry walls: an experimental research, *Materials and Structures*, **45**, pp. 1259–1276.

[7] Stavroulaki, M. & Papalou, A. (2014), Parametric analysis of old multi-leaf masonry walls, *International Journal of Conservation Science,* **5**(4), 435-446.

[8] Marcari, G; Manfredi, G; Prota, A; Pecce, M; (2007) In-plane shear performance of masonry panels strengthened with FRP. *Composites Part B: Engineering*, 2007;38:887–901.

[9] Vintzileou, E. (2011), 'Three-leaf masonry in compression, before and after grouting: A review of literature', *International Journal of Architectural Heritage* **5**(4-5), 513-538.

[10] Silva, B.; Dalla Benetta, M.; Da Porto, F. & Valluzzi, M. R. (2014), Compression and sonic tests to assess effectiveness of grout injection on three-leaf stone masonry walls, *International Journal of Architectural Heritage* **8**(3), 408-435.

[11] Silva, B.; Dalla Benetta, M.; Da Porto, F. & Modena, C. (2014), Experimental assessment of in-plane behaviour of three-leaf stone masonry walls, *Construction and Building Materials* **53**, 149-

161.

[12] Valluzzi, M. R.; Da Porto, F. & Modena, C. (2004), Behavior and modeling of strengthened three-leaf stone masonry walls, *Materials and Structures/Materiaux et Constructions* **37**(267), 184-192.

[13] Egermann, R. (1991), Experimental analysis of multiple leaf masonry wallets under vertical loading, *in* Structural Repair and Maintenance of Historical Buildings II, pp. 197-208.

[14] Drei, A. & Fontana, A. (2001), *Influence of geometrical and material properties on multiple-leaf walls behaviour*, Vol. 7.

[15] Pina-Henriques, J.; Lourenço, P. B.; Binda, L. & Anzani, A. (2004), Testing and modelling of multi-leaf masonry walls under shear and compression, *in* Proceedings of IV International Seminar on Structure Analysis of Historic Constructions, Padova, pp. 299-310.

[16] Milani, G. (2008), 'D upper bound limit analysis of multi-leaf masonry walls, *International Journal of Mechanical Sciences* **50**(4), 817-836.

[17] Milani, G. (2010), 3D FE limit analysis model for multi-layer masonry structures reinforced with FRP strips, *International Journal of Mechanical Sciences* **52**(6), 784-803.

[18] Ceravolo, R.; Pistone, G.; Zanotti Fragonara, L.; Massetto, S. & Abbiati, G. (2014), Vibration-based monitoring and diagnosis of cultural heritage: a methodological discussion in three examples, *International Journal of Architectural Heritage,* DOI: 10.1080/15583058.2013.850554.

[19] Zanotti Fragonara, L.; Boscato, G.; Ceravolo, R.; Ientile, S. & Pecorelli, M.L., (2017) Dynamic investigation on the Mirandola bell tower in post-earthquake scenarios, *Bulletin of Earthquake Engineering* **15**(1), pp. 313-337.

[20] Giaretton, M. (2011), Experimental study on the dynamic behaviour of multi-leaf stone masonry walls reinforced through injections and transversal steel ties, Master's Thesis, University of Padova 2011.

[21] Ramos J.L. (2007), Damage identification on masonry structured base on vibration signatures, PhD thesis, University of Minho 2007.

[22] Guillaume, P.; Van der Auweraer, H.; Verboven, P.; Vanlanduit, S. & Peeters, B. (2003) A poly-reference implementation of the least-squares complex frequency domain-estimator, *in* Procedings of the 21th International Modal Analysis Conference, Kissimmee (Florida).

[23] Aldeghetti, I.; Baraldi, B.; Boscato, G.; Cecchi, A.; Massaria, L.; Pavlovic, M.; Reccia, E. & Tofani, I. (2017), Multi-leaf masonry walls with full, damaged and consolidated infill: experimental and numerical analyses., *in* Murico 2017.

[24] Cecchi, A. & Sab, K. (2002), A multi-parameter homogeneization study for modelling elastic masonry, *European Journal of Mechanics A/Solids* **21**, 249-268.

[25] Reccia, E.; Milani, G.; Cecchi, A. & Tralli, A. (2014), Full 3D homogenization approach to investigate the behavior of masonry arch bridges: The Venice trans-lagoon railway bridge,

Construction and Building Materials **66**, 567-586.

[26] El-Kafafy, M.; Guillaume, P.; Peeters, B.; Marra, F. & Coppotelli, G. (2012), Advanced Frequency-Domain Modal Analysis for Dealing with Measurement Noise and Parameter Uncertainty, Topics in Modal Analysis I, Volume 5 pp 179-199.

[27] Ewins DJ. Modal testing. Research Studies Press Ltd, 2000.

[28] Lourenço, P. B.; Milani, G.; Tralli, A. & Zucchini, A. (2007), Analysis of masonry structures: Review of and recent trends in homogenization techniques, *Canadian Journal of Civil Engineering* **34**(11), 1443-1457.

[29] Bacigalupo, A. & Gambarotta, L. (2010), Second-order computational homogenization of heterogeneous materials with periodic microstructure, *ZAMM Zeitschrift fur Angewandte Mathematik und Mechanik,* **90**(10-11), 796-811.

[30] Baraldi, D.; Cecchi, A. & Tralli, A. (2015), Continuous and discrete models for masonry like material: A critical comparative study, *European Journal of Mechanics, A/Solids* **50**, 39-58.

[31] Casalegno, C.; Cecchi, A.; Reccia, E. & Russo, S. (2013), Heterogeneous and continuous models: Comparative analysis of masonry wall subjected to differential settlements, *Composites: Mechanics, Computations, Applications* **4**(3), 187-207.

[32] Trovalusci, P. & Masiani, R. (2003), Non-linear micropolar and classical continua for anisotropic discontinous materials, *International Journal of Solids and Structures*, vol. 40, no. 5, pp. 1281-1297

[33] Greco, F.; Leonetti, L.; Luciano, R. & Trovalusci, P. (2017) Multiscale failure analysis of periodic masonry structures with traditional and fiber-reinforced mortar joints, *Composites Part B: Engineering*, **118**, 75-95.

[34] Lemos, J. V. (2007), Discrete element modeling of masonry structures, *International Journal of Architectural Heritage* **1**(2), 190-213.

[35] Baraldi, D.; Bullo, S. & Cecchi, A. (2016), Continuous and discrete strategies for the modal analysis of regular masonry, *International Journal of Solids and Structures* **84**, 82-98.

[36] STRAUS7® (2004) Theoretical manual-theoretical background to the Strand7
Finite Element analysis system.